energies

Review

Solar Organic Rankine Cycle (ORC) Systems: A Review of Technologies, Parameters, and Applications

Dominika Matuszewska

Department of Thermal and Fluid Flow Machines, Faculty of Energy and Fuels, AGH University of Science and Technology, 30 Mickiewicza Ave., 30-059 Krakow, Poland; dommat@agh.edu.pl

Abstract: The Organic Rankine Cycle (ORC) is a widely utilized technology for generating electricity from various sources, including geothermal energy, waste heat, biomass, and solar energy. Harnessing solar radiation to drive ORC is a promising renewable energy technology due to the high compatibility of solar collector operating temperatures with the thermal requirements of the cycle. The aim of this review article is to present and discuss the principles of solar-ORC technology and the broad range of solar-ORC systems that have been explored in the literature. Various solar energy technologies capable of powering ORC are investigated, including flat plate collectors, vacuum tube collectors, compound parabolic collectors, and parabolic trough collectors. The review places significant emphasis on the operating parameters of technology.

Keywords: solar Organic Rankine Cycle; solar-ORC; SORC; collectors

Citation: Matuszewska, D. Solar Organic Rankine Cycle (ORC) Systems: A Review of Technologies, Parameters, and Applications. *Energies* **2024**, *17*, 5106. https://doi.org/10.3390/en17205106

Academic Editor: Antonio Rosato

Received: 11 July 2024
Revised: 14 September 2024
Accepted: 1 October 2024
Published: 14 October 2024

1. Introduction

Due to the growing global population, the rapid development of industry, and technological advancements, human economic activity is increasing significantly. This leads to a greater use of the available energy sources, with fossil fuels being the primary source of energy [1–3]. However, since fossil fuels are limited and deplete with regular use, alternative energy sources need to be sought. Moreover, the use of fossil fuels in various sectors has not only led to the depletion of energy resources but has also had a negative impact on the environment, causing greenhouse gas emissions, water acidification, and more. The inefficiency of fossil fuels, dictated by the principles of thermodynamics, results in a slow and inefficient process of combustion and energy conversion [4,5]. Research conducted by various scientists indicates that about 60% of the primary industrial energy is lost as waste heat (mostly low and medium grade thermal energy) during combustion and other heat exchange processes [6,7]. For these reasons, renewable energy is rapidly emerging as a growing and increasingly competitive alternative to fossil fuels [8,9]. Scientists have explored and proposed several thermodynamic systems and cycles for the effective utilization of low-quality heat from various sources, including various variants of the Organic Rankine Cycle and flash cycle [10–13], Goswami cycle [14,15], Kalina cycle [16,17], and some combined cycles [18–21].

Among the currently available technologies, the Organic Rankine Cycle is recognized as a promising solution for efficiently converting low- to medium-grade thermal energy into electrical power, utilizing various energy sources including solar energy [22,23], geothermal energy [24,25], industrial waste heat [26,27], biomass [28,29], and ocean thermal energy [30,31].

The Organic Rankine Cycle technology utilizes organic substances with low boiling points as working fluids to convert thermal energy into mechanical work. With hundreds of organic working fluids available, including hydrocarbons, hydrofluoroolefins, and siloxanes, selecting an appropriate fluid is crucial for ORC system design. The basic ORC process involves evaporation, expansion, condensation, and compression. However, advanced configurations like regenerative ORC, transcritical ORC, etc., have been developed to enhance performance. A key challenge in ORC system design is choosing the right working fluid from a vast array of options. This decision affects the efficiency and feasibility of the system. The cycle configuration is another critical aspect, with different configurations optimized for various heat sources to maximize thermal energy utilization [32–34].

Equally important seems to be component selection, which directly influences the system's investment cost and operational efficiency. For instance, the expansion process in ORC systems can be achieved using turbines, screw expanders, scroll expanders, or reciprocating piston expanders, each with its own cost and performance characteristics [35,36].

Operating parameters, such as temperature and pressure, also play a vital role in the ORC system's performance. Once the working fluid, cycle configuration, and components are chosen, these parameters must be optimized to achieve the best possible performance. The design process involves balancing numerous variables, making it complex and highly nonlinear.

In case of solar Organic Rankine Cycle (SORC) plants, solar collectors are used to convert solar energy into the thermal energy. The choice of solar collectors and the method of utilizing solar energy—whether through direct or indirect systems—significantly impacts system performance and must be carefully considered during the design phase of solar-ORC technology [37,38].

The ORC technology is known since 1826 when T. Howard first experimented with ether as a working fluid in a power cycle. Building on this concept, Ofeldt and Escher Wyss AG developed several naphtha engines to power launches. However, these engines were limited to niche markets due to numerous accidents that hindered the development of ORC technology at that time. The first modern example of an ORC system was created by D'Amelio in 1936. This plant utilized a simple monochloroethane Rankine cycle, heated with solar energy and powered by a single-stage impulse turbine [39].

The development of ORC technology accelerated after 1970—nowadays, more than 25 companies are working in the ORC market. In 2017, the total installed capacity reached 2749.1 MWel [40] across 563 power plants. An additional 523.6 MWel [40] was planned with the introduction of 75 new units. Geothermal power plants accounted for 76.5% of the ORC-driven capacity worldwide, followed by waste heat recovery units (including those from gas turbines, diesel power plants, and others) at 12.7%, while biomass applications made up 10.7%. The share of installed capacity of solar applications is minimal, mostly because of the high investment costs of solar fields which make ORC systems with concentrating collectors more expensive than photovoltaic (PV) panels and battery systems [40,41]. The solar-ORC plants around the world, by manufacturer, are shown in the table below (Table 1).

The primary objective of this review paper is to summarize and discuss the existing research on solar-ORC systems. This includes examining various types of solar collectors and focusing on the performance metrics of solar-ORC plants. The review aims to provide a comprehensive overview of the advancements and challenges in integrating solar energy with ORC technology, highlighting the potential for these systems to contribute to a more sustainable energy landscape. In summary, the design of solar-ORC systems involves several critical considerations. The selection of the appropriate solar collectors and the decision between the direct and indirect solar energy utilization methods are fundamental to optimizing system performance. With solar energy being a sustainable and abundant resource, its integration with ORC technology offers significant potential for efficient and sustainable energy production. This review seeks to encapsulate the current state of research in this field, providing insights into the effectiveness and prospects of solar-ORC systems.

The aim of this review article is to present and discuss the principles of solar-ORC technology and the broad range of solar-ORC systems that have been explored in the literature. The contribution of this study was to provide a review on the performance of the operating parameters of solar-ORC technologies powered by various solar energy technologies including flat plate collectors, vacuum tube collectors, compound parabolic collectors, parabolic trough collectors, and linear Fresnel reflectors. The article is structured as follows: Section 2 describes the ORC system with the working fluid (WF) selection and model description. Section 3 presents heat source specification and the introduction of solar collector options for ORC technology. Section 4 puts emphasis on solar-ORC systems with different types of solar collector options and their operating parameters. Finally, Section 5 contains the conclusions.

Table 1. Solar-ORC construction in the world according to manufacturers. Based on [40].

Country	Site Plan	Company	Capacity	Year
Australia	Mulka Bore	Enreco	15 kWel	1975
Australia	Mulka Station	Enreco	15 kWel	1980
Germany	Schleiz	GMK	150 kWel	2005
USA	APS	ORMAT	1000 kWel	2006
USA	Kona, Hawaii	Electratherm	50 kWel	2009
Morocco	Ait Baha	Turboden	2000 kWel	2010
USA	Lafayette	Electratherm	65 kWel	2012
Spain	Heliotec	RANK	2.5 kWel	2012
Brazil	Itajuba	ENOGIA	10 kWel	2013
USA	Tampa	Electratherm	65 kWel	2014
Burkina Faso	Ouagadougou	ENOGIA	10 kWel	2014
France	Odeillo	ENOGIA	20 kWel	2015
Italy	Palermo	RANK	10 kWel	2015
Italy	UniKore	Zuccato	50 kWel	2015
Greece	Xanthi	ENOGIA	10 kWel	2015
Egypt	Cairo	ENOGIA	10 kWel	2015
India	Rainbow	ENERTIME	100 kWel	2015
Qatar	Gord	ENOGIA	10 kWel	2016
Tunisia	Tunisia	Zuccato	60 kWel	2016
Turkey	Bricker	RANK	87 kWel	2016
China	Confidential	ENOGIA	10 kWel	2016
France	Solho	RANK	1.5 kWel	2018
Denmark	Bronderslev	Turboden	3800 kWel	2018
Spain	Magtel	RANK	11 kWel	2019
Spain	Soria	Enerbasque	3 kWel	2019
Spain	Almeria	ENOGIA	10 kWel	2020
Slovakia	Lehnice	ENOGIA	10 kWel	2022

2. Description of the Organic Rankine Cycle

A simple ORC system consists of several key components (Figure 1) as follows: a heat recovery system (HRS), an expander, a condenser, and a pump. The marked numbers in the Figure 1 correspond to the points marked in the thermodynamic process of ORC cycle diagram shown in Figure 2.

In the heat recovery system (HRS), heat exchange processes between the heat source (solar collectors) and the working fluid occur in the following three main sections: the superheater, evaporator, and preheater. The temperature of the heat source gradually decreases from A to D, while the temperature of the working fluid increases from 5 to 1.

First, heat from the heat source is transferred to the working fluid in the superheater. During this process, saturated vapor (state 7) is heated into superheated vapor (state 1), with the heat source temperature dropping from A to B. In the ORC cycles, the superheating section is usually small (increasing vapor temperature by 5–10 K) or even omitted in case of dry refrigerants due to the positive slope of the T-s curve. Next, in the evaporator, the phase change of the working fluid occurs; the saturated liquid (state 6) turns into saturated vapor (state 7), while the temperature of the heat source drops further from B to C. Finally, in the preheater, the subcooled liquid (state 5) is heated to become a saturated liquid (state 6), and the heat source temperature reaches its lowest value, D.

This entire process ensures a gradual transfer of heat from the collectors to the working fluid, increasing its enthalpy and enabling the efficient conversion of thermal energy into mechanical energy within the ORC cycle.

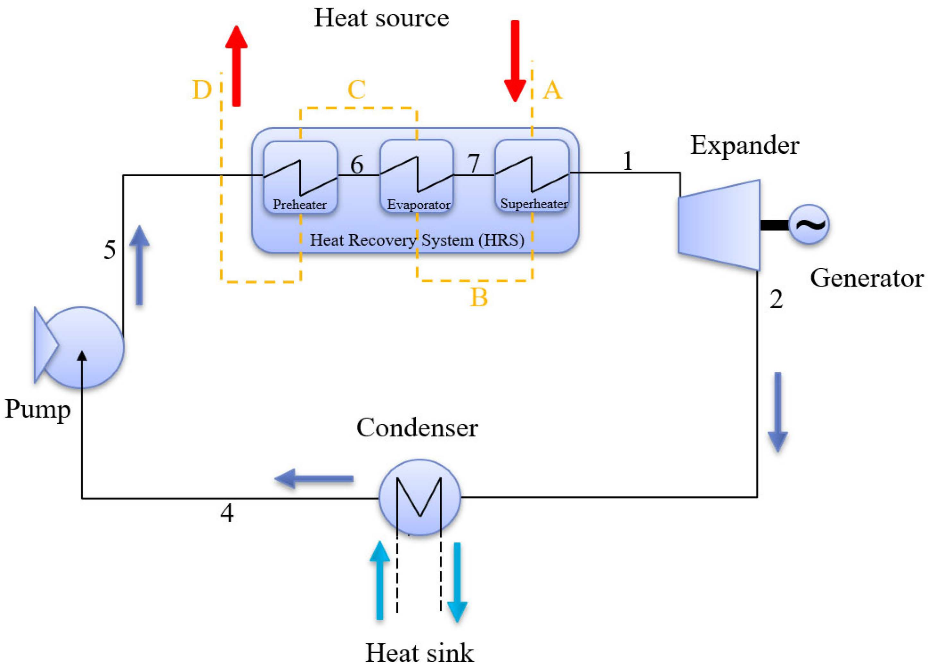

Figure 1. Basic ORC system with key component and state-point notations.

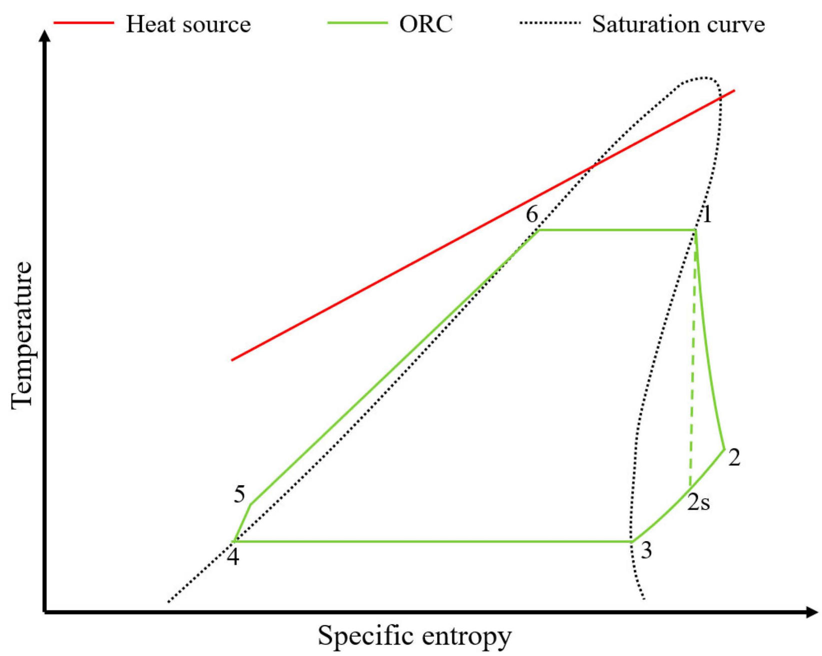

Figure 2. Temperature-specific entropy diagram of an ORC system.

In the expander, the superheated vapor (state 1) is expanded to the lower pressure (state 2). Following this, the vapor moves to the condenser, where heat is rejected to the ambient environment, condensing the vapor into a low-pressure saturated liquid (state 4). The heat rejection process in an ORC cycle, which occurs in the condenser, can be divided into the following two distinct stages (2–4): desuperheating, during which the temperature decreases at a constant pressure (2–3), and condensation, where the phase change of the working fluid occurs at constant pressure (3–4). The pump increases the pressure of the saturated liquid (up to state 5) and then liquid enters the HRS, where it is preheated, evaporated, and superheated.

Figure 3 shows the temperature–heat transfer in the HRS, which highlights the importance of the pinch point in the system's design. The pinch point is the minimum temperature difference between the heat source stream and the working fluid within the HRS, typically ranging from 5 K to 20 K. This critical parameter can occur in the following three possible locations within the HRS: the preheater inlet, between the preheater and evaporator, and at the outlet of the superheater. The location of the pinch point varies based on the temperature of the heat source. For high-temperature heat sources, the pinch point is usually at the preheater inlet. Conversely, for low-temperature heat sources, it tends to be at the superheater outlet. Most commonly, the pinch point is situated between the preheater and the evaporator. The position of the pinch point significantly affects the design and efficiency of the HRS. It dictates how effectively heat can be transferred from the heat source to the working fluid. By minimizing the temperature difference at the pinch point, the system can maximize heat recovery efficiency, leading to the better overall performance of the ORC unit.

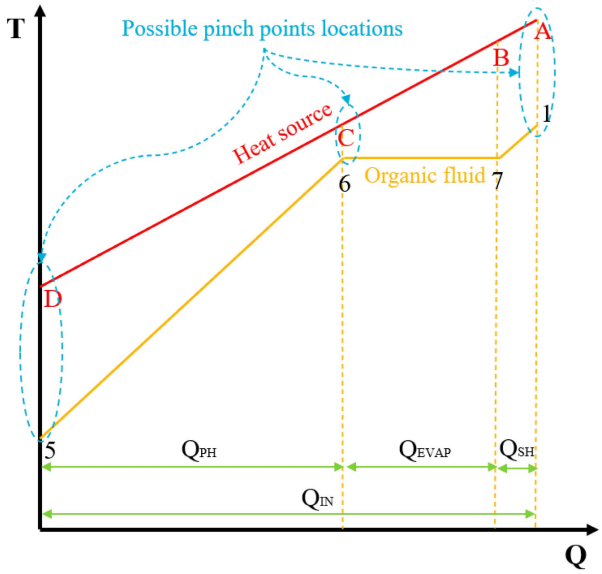

Figure 3. Temperature–heat diagram for preheater, evaporator, and superheater.

In summary, the basic ORC system operates through a sequence of heat addition, expansion, heat rejection, and pressurization processes, facilitated by the HRS, turbine, condenser, and pump, respectively. Understanding the thermodynamic processes and the critical role of the pinch point in the HRS helps optimize the design and efficiency of the ORC systems. These insights contribute to the development of more effective and sustainable energy conversion technologies.

2.1. Working Fluid Selection

Organic working fluids used in ORC systems can evaporate at much lower temperatures compared to water in water–steam Clausius–Rankine cycles. Additionally, they very often do not require superheating (or required heating by 5–10 K). To produce mechanical power, these organic fluids undergo expansion in a turbine or expander, with the expansion dynamics being highly influenced by process conditions such as the initial thermodynamic state and expansion ratio.

Various requirements, closely tied to the specific application of the ORC, drive the selection of working fluids in the ORC systems; those include the temperature of the heat source, fluid compatibility, flammability, toxicity, and environmental impact. Typically, ORC fluids are organic chemical fluids with high molecular weights, significantly lower critical temperature and pressure than water, very often with a slope shape that eliminates the need for superheating. These characteristics make them suitable for utilizing low- and medium-temperature heat sources.

However, there are challenges in selecting ORC fluids. These include incomplete data on their thermal properties, difficulties in finding suitable replacements for older, environmentally harmful fluids, and ensuring compatibility with the existing systems [42].

Organic fluids can be categorized into three groups based on the shape of their saturation lines—wet, isentropic, and dry. The shape of the saturation line is crucial in ORC plant design and equipment selection, as it significantly impacts system efficiency. Dry and isentropic fluids are highly recommended for ORC plants as they either do not require superheating or only require minimal superheating thus reducing the risk of turbine blade corrosion. Of the two, isentropic fluids are preferred since they eliminate the need for a regenerator. In an ORC system with isentropic fluids, the saturated vapor at the turbine inlet expands along a vertical line and remains saturated when exiting the turbine [42,43].

Recent research is focused on the impact of the molecular characteristics of organic fluids and the dense-gas flow phenomena, which are not well understood at present. Heavy organic fluids used in ORC systems have complex molecular structures, leading to non-classical behavior near the saturated vapor curve ($x = 1$). Therefore, it is crucial to study and analyze the measures of fluid complexity and their impact on fluid behavior and parameters. By understanding molecular complexity, the slope shape of the saturation vapor curve can be predicted, indicating whether a fluid is wet (negative slope), isentropic, or dry (positive slope). The coefficient σ, typically referenced at a reduced temperature $Tr = 0.7$, can be used for this purpose, as defined by the following equation [44]:

$$\sigma_{Tr=0.7} = \frac{T_c}{R} \cdot \left(\frac{ds}{dT} \right)_{x=1} \quad (1)$$

The σ coefficient, a function of heat capacity, is closely linked to the molecular structure of the fluid. As molecular complexity rises, a decrease in the heat capacity ratio γ is noted. This results in a positive slope of the saturation vapor curve; the more positive the slope, the greater the molecular complexity (Figure 4).

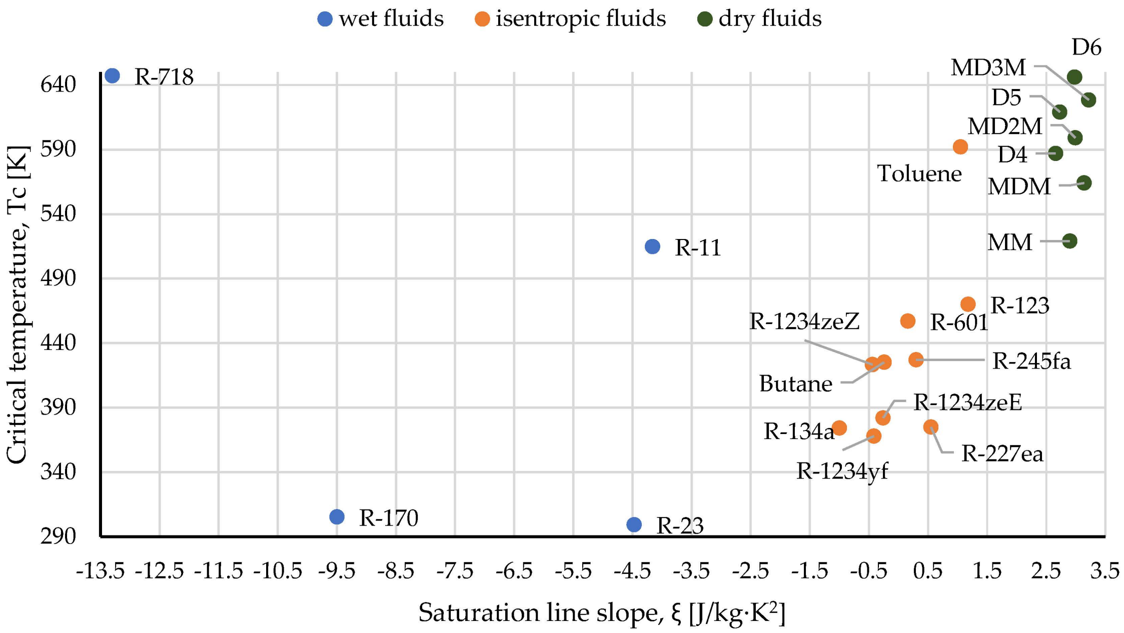

Figure 4. Some of the wet, isentropic, and dry fluids using in ORCs.

In the literature, there is a lot of research in the context of working fluid selection or use in solar-ORC systems. Tchanche et al. [45] analyzed the use of 20 different working fluids in low-temperature solar collectors used with ORC. Under their conditions, R134a was the most suitable. Almehmadi et al. [46] investigated three innovative solar-driven poly-generation systems (BS, IS-I, and IS-II) combined with an ORC, a humidification–dehumidification desalination system (HDH), and a desiccant cooling system (DCS). The research analyzed the effects of different operating conditions and organic working fluids on system performance, demonstrating significant efficiency improvements and highlighting the superior performance of the IS-I system and the advantages of using fluids like n-octane and R113. Loni et al. [47] research investigated the performance of three nanofluids (Al_2O_3/oil, CuO/oil, and SiO_2/oil) in hemispherical, cubical, and cylindrical receivers, with methanol as the ORC working fluid. The study revealed that while nanofluids slightly improved the thermal efficiency of the cavity receivers, the cubical receiver using Al_2O_3/oil nanofluid emerged as the most efficient configuration for the solar-ORC system. Jiang et al. [48] assessed the performance of direct vapor generation ORC (DVG-ORC) systems under various conditions, comparing traditional fluids with low global warming potential alternatives. Results indicate that R1336mzz (Z) was highly suitable, showing only a slight decrease in the net output power compared to R245ca while offering superior ORC and system efficiency, making it an environmentally friendly and efficient choice for DVG-ORC systems. In their study, Rayegna and Tao [49] introduced a systematic approach for selecting the optimal working fluids in solar-ORC systems under comparable operating conditions. Their methodology involved evaluating various parameters including molecular composition, temperature–entropy characteristics, and impacts on thermal efficiency, net power output, vapor expansion ratio, and exergy efficiency. From their findings, they identified eleven promising working fluids suitable for use in low- to medium-temperature solar-ORC applications.

In summary, the extensive literature emphasizes the complexity of ORC working fluid selection beyond thermodynamic and thermal properties, highlighting the additional critical factors. Environmental impacts, including global warming potential and ozone depletion potential, alongside considerations of toxicity and flammability, are pivotal in fluid choice. Furthermore, the chemical stability of the working fluid is crucial, as it sets constraints on the maximum achievable heat source temperature, underscoring the comprehensive nature of fluid selection criteria in the ORC systems [44,50].

2.2. Modeling

The rate of heat transfer in the HRS ($\dot{Q}_{IN}$) can be determined using the energy balance of the control volume of the working fluid:

$$\dot{Q}_{IN} = \dot{m}_{WF} \cdot (h_1 - h_5) \tag{2}$$

where the following terms are used:

- $\dot{m}$ represents the mass flow rate in kg/s,
- h represents the specific enthalpy in kJ/kg.

The heat exchange between the solar energy and the organic working fluid occurs in both the preheater ($\dot{Q}_{PH}$), the evaporator ($\dot{Q}_{EVAP}$) and the superheater ($\dot{Q}_{SH}$). The energy balance equations that describe this process in those components are given by the following relations:

$$\dot{Q}_{PH} = \dot{m}_{WF} \cdot (h_6 - h_5) \tag{3}$$

$$\dot{Q}_{EVAP} = \dot{m}_{WF} \cdot (h_7 - h_6) \tag{4}$$

$$\dot{Q}_{SH} = \dot{m}_{WF} \cdot (h_1 - h_7) \tag{5}$$

The power generated in the turbine ($\dot{W}_T$) is calculated based on the following equation:

$$\dot{W}_T = \dot{m}_{WF} \cdot (h_1 - h_2) \tag{6}$$

Considering the mechanical efficiency (η_m) and the efficiency of generator (η_g), the electricity production by the shaft (P_{EL}) refers to the following equation:

$$P_{EL} = \eta_m \cdot \eta_g \cdot \dot{W}_T \tag{7}$$

The internal efficiency of the turbine is modelled according to the following equation:

$$\eta_{iT} = \frac{h_1 - h_2}{h_1 - h_{2s}} \tag{8}$$

where h_2 is the real state of turbine and h_{2s} is corresponding state for the isentropic case.

The rate of heat rejected ($\dot{Q}_{OUT}$) from the condenser is modeled based on the following equation:

$$\dot{Q}_{OUT} = \dot{m}_{WF} \cdot (h_2 - h_4) \tag{9}$$

The pump power consumption ($\dot{W}_P$) is calculated considering the efficiency of the motor η_{motor} as follows:

$$\dot{W}_P = \frac{\dot{m}_{WF} \cdot (h_5 - h_4)}{\eta_{motor}} \tag{10}$$

The net electricity produced by the ORC system ($P_{EL,NET}$) refers to the power generated by the turbine reduced by the pump power consumption as in the following equation:

$$P_{EL,NET} = P_{EL} - \dot{W}_P \tag{11}$$

The efficiency of the ORC (η_{ORC}) refers to the following equation:

$$\eta_{ORC} = \frac{P_{EL,NET}}{\dot{Q}_{IN}} \tag{12}$$

It is important to understand that the heat input in the ORC ($\dot{Q}_{IN}$) is not the same as the total heat source input in the system ($\dot{Q}_{HS}$). The heat source input exceeds the heat input in the ORC unit due to unavoidable thermal losses in the intermediate devices, resulting in $\dot{Q}_{HS}$ being greater than $\dot{Q}_{IN}$. This efficiency (η_{TH}) accounts for the losses in the intermediate devices and gives a measure of how effectively the system is utilizing the total heat available, as in the following equation:

$$\eta_{TH} = \frac{\dot{Q}_{IN}}{\dot{Q}_{HS}} \tag{13}$$

The total system efficiency (η_{SYS}) is given by the following equation:

$$\eta_{SYS} = \frac{P_{EL,NET}}{\dot{Q}_{HS}} = \eta_{ORC} \cdot \eta_{TH} \tag{14}$$

Another essential parameter for accurately characterizing the ORC unit is exergy efficiency. Exergy efficiency effectively assesses the quality of the heat source. The exergy efficiency of the system can be expressed as follows:

$$\eta_{EX.SYS} = \frac{P_{EL,NET}}{\dot{Q}_{HS} \cdot \psi_{HS}} \tag{15}$$

The exergy factor of the heat source (ψ_{HS}) varies based on the type of energy source. To account for the fact that the sun acts as a radiation reservoir rather than a heat reservoir, various correlations can be employed. Petela correlation is recommended for use in this kind of system as follows [51]:

$$\psi_{HS} = 1 - \frac{4}{3} \cdot \frac{T_{AM}}{T_{SUN}} + \frac{1}{3} \cdot \left(\frac{T_{AM}}{T_{SUN}} \right)^4 \tag{16}$$

where the following terms are used:

- T_{AM} is the temperature of the environment,
- T_{SUN} is the temperature of the sun (and is taken as 5800 K in calculations).

3. Solar Energy as Heat Source and Solar Collector Options for Its Conversion

Solar energy constitutes the predominant renewable energy source, with approximately 1×10^5 TW reaching Earth's surface. As such, it is widely accessible across various regions and stands as the best and environmentally friendly option for future electricity generation [52]. Solar-ORC systems seem to be a reliable technology to convert solar heat into electricity. The compatibility between solar systems and ORC units derives from the ORC's optimal operation within temperatures ranging up to 400 °C or 500 °C, aligning seamlessly with solar energy characteristics. Furthermore, ORC engines demonstrate adaptability across a wide spectrum of heat source temperatures, from 80 °C to 500 °C, facilitating their coupling with diverse solar collector technologies. This versatility extends to both flat solar technologies and concentrating solar technologies.

Research by Barber [53] has extensively examined the efficiency and feasibility of solar-ORC systems for electricity generation. Their findings indicate that for SORC, the optimal operating temperatures vary for different types of collectors; they obtained 93 °C for flat plates, 150–200 °C for concentrators, and 315 °C for tracking concentrators. They emphasized that low-cost collectors are essential for making SORC systems commercially viable.

In the paper, the author focused on solar-ORC systems coupled with flat collectors or with a low-concentration collector such as flat plate collectors (FPCs), evacuated tube collectors (ETCs), and compound parabolic collectors (CPCs), as well as linear concentrating collectors such as parabolic through collectors (PTCs) (Figure 5).

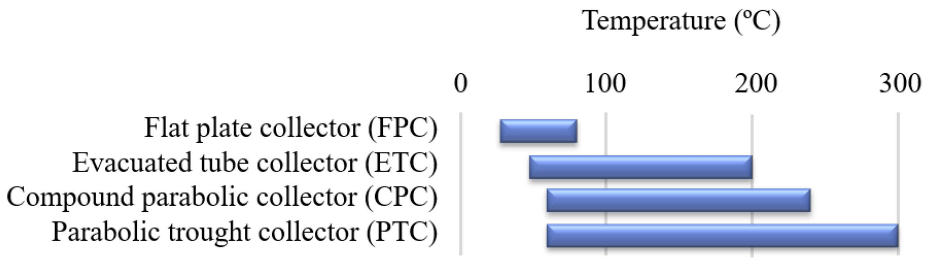

Figure 5. Temperature ranges typical for different solar thermal collectors [54].

Flat-Plate Collector (FPC). FPCs are the second solar thermal technology in terms of the installed capacity of 136.4 GW_{th}, of which 51 GW_{th} is in China. The area is 195 million m^2 [55]. These collectors produce heat mainly in the temperature range of 30 (e.g., swimming pool applications) to 100 °C. They consist of an absorber with a selective coating for solar radiation and tubes transporting heat using water or glycol solution (depending on the climate). Compared to the other types of devices, FPC solar thermal collectors are characterized by relatively high heat losses, which means that they are rarely used for purposes other than the production of domestic hot water. Their advantage compared to collectors concentrating solar radiation is that their absorbers absorb both direct and diffuse solar radiation [56,57]. They do not require tracking to function properly, although tracking increases their productivity.

Evacuated Tube Collector (ETC). It is the most frequently used solar thermal technology in the world in terms of the installed capacity of 372.9 GW_{th}, which consists of over

532 million m^2 of collector area [55]. Due to the heat loss coefficients, these collectors can generate heat usually up to 200 °C (depending on climatic conditions). Like FPCs, the absorbers absorb both direct and diffuse solar radiation and do not require tracking to function properly, although tracking increases their productivity. ETCs most often consist of two coaxial pipes, between which there is a layer of the so-called vacuum constituting thermal insulation, and a layer of selective absorber is sprayed outside the inner pipe. There are also designs with an absorber located on a flat metal element inside a single pipe [57–59].

Compound Parabolic Collector (CPC): CPCs are integrated ETC collectors with a parabolic-shaped reflector (several parts [60]). The use of a reflector makes direct solar radiation more important because only such radiation is reflected directionally onto the tube absorber within the ETC. The radiation concentration coefficient is usually around three and the operating temperature is up to 200 °C [61–64].

Parabolic Trough Collector (PTC): This is a technology based on concentrating solar radiation with a factor of 10 to 50 (up to 90 [65]), thanks to which the temperature can reach 500 °C. The concentration factor means that practically only direct solar radiation is used, which at least partially limits the regions of the world in which they can be used. Due to its design, at least one-axis tracking following the apparent movement of the sun is recommended. Additionally, PTCs from the above-mentioned types of collectors are distinguished using different working fluids, such as thermal oil, steam, or molten salts [66,67].

4. Solar-ORC Systems

Solar energy exhibits adaptability in terms of heat conversion across different temperature ranges, depending on the specific technology. The literature extensively covers studies on the solar-ORC systems employing both non-concentrating technologies and concentrating technologies. As mentioned earlier, solar-ORC systems can be divided into direct and indirect types.

In direct solar-ORC systems (Figure 6), collectors are used to directly heat the working fluid in an ORC unit. These systems are often integrated with flat-plate collectors or linear concentrating collectors, where the working fluid is heated directly by the solar thermal collectors. The direct approach simplifies the system but is generally more suited for applications requiring lower temperature ranges.

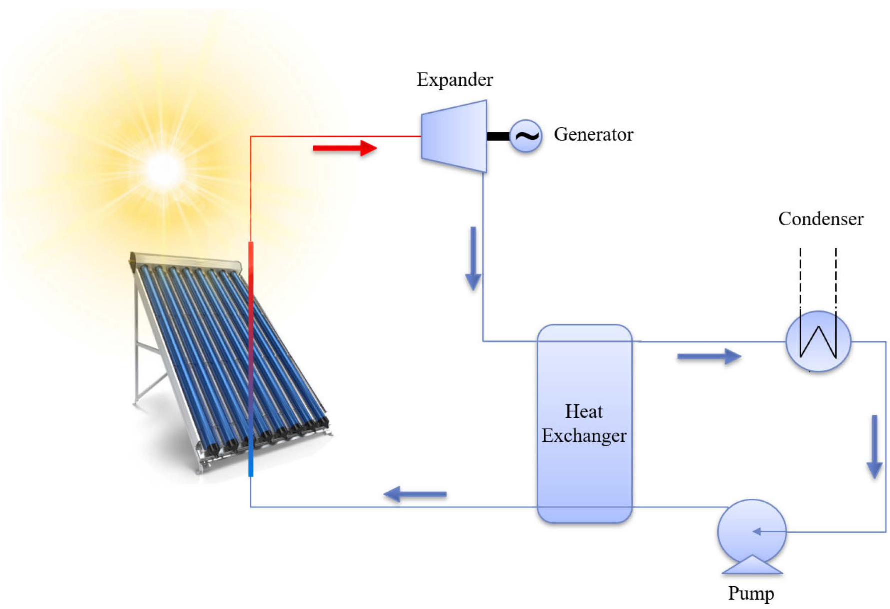

Figure 6. Schematic layout of a direct solar-ORC system.

Indirect solar-ORC systems (Figure 7), on the other hand, use a thermal energy storage (TES) or transfer medium between the solar collectors and the ORC. This method typically involves using a heat transfer fluid (HTF) or thermal storage to absorb solar energy before transferring it to the ORC system. This approach allows for better management of solar energy variability and higher operational flexibility, often accommodating higher temperature ranges.

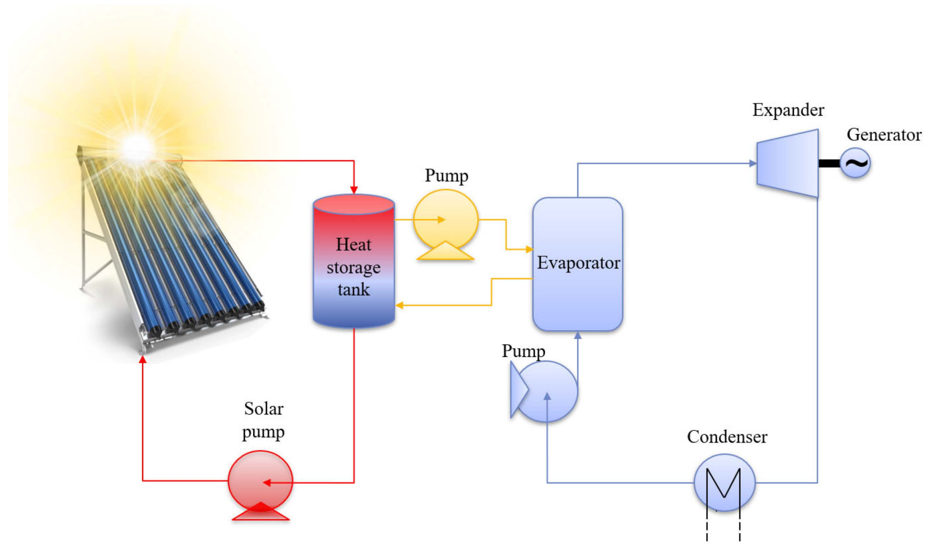

Figure 7. Schematic layout of indirect solar-ORC system.

Concentrating collectors enable operations at higher temperature ranges, thereby enhancing the thermodynamic efficiencies of the ORCs. However, utilizing these technologies also introduces challenges such as sun tracking and efficient heat storage. This section provides a comprehensive review and analysis of all the relevant studies found in the literature, offering detailed insight into these studies and ranking them with the solar thermal collectors used in the systems. The analysis is focused on the following two groups of collectors: flat collectors or with a low concentration and linear concentrating collectors. The review pays particular attention to the operating parameters of such systems.

4.1. Flat Plate Collectors (FPCs)

This section presents a literature review on the FPC-ORC technologies. Table 2 provides a summary of the main parameters of the discussed FPC-ORC units. Wang et al. [68] introduced a regenerative ORC for harnessing solar energy at low temperatures. Mathematical models are developed to simulate the system under steady-state conditions, enabling the parametric analysis of various thermodynamic parameters and their impact on system performance with different working fluids. The system is further optimized using a genetic algorithm, aiming to maximize daily average efficiency under specified conditions.

Table 2. An overview of the solar-ORC systems employing FPCs.

Region	Collector Area [m^2]	HTF	Operating Temperature [°C]	ORC System, Working Fluid	Power Output	TES Type	Authors (Year), Ref.
China (Xi'an city)	528	water	range: (50–70)/(20–30)	regenerative ORC; WFs: R245fa, R123, isobutane, R134a.	output parameters	a thermal storage system	Wang et al., 2013 [68]
Colombia (Las Flores)	optimization variables: 150–200	Thermal oil	250/(40–60)	regenerative and basic ORC; WF: toluene	output parameter	thermal storage tank volume: 50 m^3	Ochoa et al., 2023 [69]
Greece (Athens)	60	a mixture of water-glycol	range (80–100)/(55–60)	basic ORC; WFs: R245fa and R1233zd	output parameters: 0.4–0.5 kW	water tank	Ramos et al., 2018 [70]
Greece (Athens, Thessaloniki), Turkey (Istanbul), Cyprus (Larnaca)—the South-East Mediterranean region:	optimization variable	water	90/70	a single stage conventional ORC; WFs: R134a, R245fa, R227ea, R152a, R236ea, R1234ze(E)	5 kW	storage tank	Roumpedakis et al., 2020 [71]
Greece (Northern part)	144	water	output parameter/30	simple ORC: WF: several mixtures	1 kWe	the heat storage tank with capacity to 3960 l	Mavrou et al., 2015 [72]
Italy (Bologna)	21.5, 32.25, 64.5	water	range: (45–95)/(14–28)	recuperative ORC; WFs: R134a, R1234yf, R1234ze(E), R1243zf, R513A, R515A	output variable: 0–1800 W	two storage tanks varied from 0 to 12,000 L with a step of 3000 L	Ancona et al., 2022 [73]
Germany (southern part—Bayern region)	optimization of the collector area	a mixture of water-glycol	optimization: 70–90/output parameter	direct ORC system; WF: zeotropic mixtures	1 kWe	none-direct utilization	Habka and Ajib, 2016 [74]
Pakistan (Lahore)	Not Available (N/A).	water	N/A	subcritical ORC, WF: R123	17.4–40.4 kW	the PCM tank (capacity of 90 m^3)	Alvi et al., 2022 [75]
Spain (Sevilla)	output parameters	water	90/20	simple ORC, WF: R245fa	1 kW	0.3 m^3 the storage tank with six stratification levels	Rodriguez-Pastor et al., 2022 [76]
Thailand (Bangkok)	2.08 per unit, respectively; 100 to 1200 units (with 50 units increment)	water	N/A	simple ORC; WF: R245fa	20, 40 and 60 kWe	none	Sonsaree et al., 2018 [77]
United Kingdom	550	water	(70–105)/30	basic ORC; WF: R245fa	output parameter: ranged from 4.3 to 5.7 kW in the daytime, 9 to 11.2 kW at early night and 4.7 to 4.3 kW in night	pressurized water storage unit	Kutlu et al., 2018 [78]
United Kingdom (London)	15	Therminol VP-1	180/40	six different ORC configuration; WFs: sixteen working fluids	0.8–3 kW	two-tank configuration (high temperature, low temperature), buffer	Wang et al., 2021 [34]

Ochoa et al. [69] provided a thermo-economic and environmental performance optimization of the regenerative Organic Rankine Cycle and the Simple Organic Rankine Cycle using Particle Swarm Optimization (PSO). Their research focused on optimizing the collecting area of basic and regenerative ORC systems in Colombia. Also, Ramos et al. [70], in their research, focused on optimizing the system consisting of a set of solar collectors, an ORC system, and a storage system. The focus was on determining the operating conditions of the system and maximizing the output power. In their work, they optimized a basic ORC system connected to different types of collectors, including an FPC and ETC, and working under different conditions. Installation with an FPC operated in a temperature range of between 100 and 80 °C and 60 and 55 °C, while those with an ETC operated in a range of between 200 and 180 °C and 60 and 55 °C. These values, in turn, affected the power output range, which varied from 0.4 to 0.5 kW and from 1.2 to 1.8 kW, respectively. Additionally, the optimization of the solar field area for both the FPC and ETC collectors, as well as the volume of the storage tank from an economic and thermodynamic perspective, was carried out by Roumpedakis et al. [71]. Their work considered the optimization of small-scale, low-temperature, solar-driven ORCs using various types of solar collectors and working fluids (R1234ze(E), R134a, R152a, R227ea, R236a) for the following four distinct locations: Athens (Greece), Istanbul (Turkey), Larnaca (Cyprus), and Thessaloniki (Greece). A genetic algorithm was used to minimize the payback period and maximize the exergy efficiency. For FPCs functioning at a temperature of 90 °C, R245fa was found to be the most efficient working fluid with an efficiency of 5.4%. Mavrou et al. [72] explored the performance of working fluid mixtures in solar-ORC systems with heat storage using an FPC. Their work examined the impact of heat source variability on ORC performance with different fluid mixtures. Through a multi-criteria mixture selection methodology, they determined the optimum operating ranges for generating 1 kW of power efficiently. Ancona et al. [73] provided an estimation of electricity production from a solar recuperative ORC system dedicated for a single-family home evaluated based on the experimental data. Habka and Ajib [74] estimated and compared the efficiency of zeotropic mixtures and pure fluids in two variants of mini-solar cogeneration units using the ORC. The focus was on optimizing and evaluating these systems based on the energy and economic criteria. Alvi et al. [75] investigated the influence of phase change materials (PCM) in the storage system on the efficiency of the collectors and ORC unit, power, temperature, and heat storage in a direct vapor generation solar-ORC system. Rodriguez-Pastor et al. [76] evaluated the advantages and disadvantages of variability in the demand and availability of solar resources for the purposes of solar-ORC integration in residential buildings. Parametric (including solar field, storage volume, and productivity analysis) and thermo-economic analysis were added. Sonsaree et al. [77] investigated the utilization of low-temperature heat (under 100 °C) from solar energy using ORCs with different capacities (20, 40, and 60 kWe). Three different types of collectors were analyzed—CPCs, ETCs, and FPCs. The mathematical model created by the authors evaluated the maximum output power and CO_2 emissions, and they conducted an economic analysis in terms of the levelized cost of electricity (LCOE). The results showed that the system combined with CPC collectors could produce a higher power output (compared to systems with the same number of different type collectors). Kutlu et al. [78] investigated a medium-temperature solar-ORC system using evacuated flat-plate collectors and a pressurized water storage unit. The primary objective was to analyze the system's performance, considering the transient behavior of the thermal storage unit and its impact on other components. Moreover, the study aimed to optimize the power output to align with the varying electricity demand throughout the day. Wang et al. [34] investigated thermodynamic and economic performance for small-scale domestic solar-ORCs. They analyzed the following different configurations of solar-ORC cycles: subcritical nonrecuperative ORCs (SNORCs), subcritical recuperative ORCs (SRORCs); transcritical nonrecuperative ORCs (TNORCs); transcritical recuperative ORCs (TRORCs), trilateral ORCs (TLCs), and partial evaporation ORCs (PECs). Each configuration was evaluated for the following sixteen different organic fluids: R1234yf, R1234ze, R152a, isobutane, butane, R245fa, R1233zd, R245ca, isopentane, pentane, R125, R143a, R32, R404a, R410a, and R407c. It is worth noting that, in the conducted study, only the area of the solar panels was constant, corresponding to the average roof area available in houses in United Kingdom for such installations (15 m^2) and the design parameters of the proposed tanks, which had a storage capacity corresponding to 5 h of operating time. The sizes of the other individual elements of the installation were optimized and adapted to the different analyzed fluids and installation configurations. The study found that the solar-ORC systems based on an SRORC with evacuated flat-plate collectors, piston expanders, and isobutane as the working fluid outperformed other designs in thermodynamic performance. The system generated 1100 kW·h/year (73 kW·h/year/m^2) of electricity, with an overall thermal efficiency of 5.5%.

4.2. Evacuate Tube Collectors (ETCs)

The ETC is typically a stationary collector employed in low and medium temperature applications. Unlike FPCs, ETCs can operate at temperatures exceeding 100 °C, which is a significant advantage. However, this technology comes with higher investment costs. The literature provides various analyses about the combination of ETCs with ORCs. Table 3 presents a summary of the main parameters of the discussed ETC-ORC units.

Twomey et al. [79] tested the spiral expander on a small ETC-ORC system and then used it to calibrate the static expander model. This calibrated model was then used for a larger dynamic model designed for a larger residential unit (hotels, senior citizen homes, and multiple dwelling houses) or a small commercial facility. Piñerez et al. [80] conducted an energy, exegetical, and environmental analysis of a simple ORC system driven by a solar collector, with a vacuum tube integrated with a heat accumulator. It was found that the highest thermal stability of the working fluid in the ORC is obtained when the heat from the storage tank is released during hours without radiation. Gilani et al. [81] analyzed the solar-ORC system used to power air-conditioning with the power generated per year at 8154 kWh/year. Bellos et al. [82] provided an optimization of the regenerative solar-ORCs working with and without recuperative heat from evacuated tube collectors (ETCs). The novel design of a solar-ORC system increased the energy efficiency (from 5.1 to 7%) and financial performance compared to the normal usual regenerative system. Scardigno et al. [83] presented the multi-objective optimization of a hybrid organic Rankine plant that utilized solar and low-grade energy sources. The primary goal was to identify solutions that maximize the efficiencies based on both the first and second laws, while simultaneously minimizing the levelized energy cost (LEC). To achieve this, the study used NSGAII—a non-dominated sorting genetic algorithm. Atiz et al. [84] designed a comprehensive renewable energy system to evaluate the production of electricity and hydrogen. The system included evacuated tube solar collectors (ETSCs) with a total surface area of 300 m^2, a salt gradient solar pond (SGSP) covering 217 m^2, an ORC, and an electrolysis unit. Heat stored in the heat storage zone (HSZ) was transferred to the input water of the ETSCs via a heat exchanger, allowing the ETSCs to further elevate the temperature of the preheated water, which significantly enhanced the ORC's performance. The system's balance equations were formulated and analyzed using the Engineering Equations Solver (EES) software. Consequently, the overall system's energy and exergy efficiencies were determined to be 5.92% and 18.21%, respectively. Additionally, the system's hydrogen production capacity was found to be up to 3204 g per day. The achieved overall system efficiency/hydrogen production values were surprisingly low, especially considering the complexity of the system and the efficiency of devices such as ETCs.

Table 3. An overview of the solar-ORC systems employing ETCs.

Region	Collector Area [m^2]	HTF	Operating Temperature [°C]	ORC System, Working Fluid	Power Output	TES Type	Authors (Year), Ref.
Australia (Brisbane)	50	water	85–120/output data	simple ORC (with scroll expander); WF: R134a	output data: max. instantaneous power is 676 W	solar storage vessel with water (800 L)	Twomey et al., 2012 [79]
Colombia (cities Rancho Grande, Puerto Bolivar, Manaure, and Nazareth)	100	thermal oil Therminol 75	(120–130)/20	simple ORC WFs: Toluene, Cyclohexane, and Acetone	design output: 3–7.5 kW	a thermal storage tank: a storage tank that operates during non-radiation hours	Piñerez et al., 2021 [80]
Cyprus (Paralimni)	265	water	95/40	simple and internal heat exchange ORC; WF: isobutene	3.92 kW	storage tank capacity (optimized): 48 m^3	Gilani et al., 2022 [81]
Greece (Athens)	300	thermal oil Therminol VP-1	(80–150)/(24–45)	regenerative ORC with and without reheating; WF: cyclopentan	25, 20, 15, 10 kW	sensible thermal storage tank (5 m^3)	Bellos et al., 2022 [82]
Greece (Athens)	60	thermal oil Therminol 66	(180–200)/(55–60)	basic ORC; WFs: R245fa and R1233zd	output parameters: 1.2–1.8 kW	water tank	Ramos et al., 2018 [70]
Greece (Athens, Thessaloniki), Turkey (Istanbul), Cyprus (Larnaca)—the South-East Mediterranean region:	optimization variable	water	110/90	a single stage conventional ORC; WFs: R134a, R245fa, R227ea, R152a, R236ea, R1234ze(E)	5 kW	storage tank	Roumpedakis et al., 2020 [71]
Italy (Florence)	output parameter	water	90/output parameter	simple ORC cycle; WFs: R32, R41, R125, R134a, R143a, R152a, R218, R227ea	output parameter	none	Scardigno et al., 2015 [83]
Thailand (Bangkok)	2.37 per unit, respectively; 100 to 1200 units (with 50 units increment)	water	N/A	simple ORC; WF: R245fa	20, 40 and 60 kWe	none	Sonsaree et al., 2018 [77]
Turkey (Adana)	300	water	90/39	simple ORC system; WF: isobutan	output data	none	Atiz et al., 2018 [84]
United Kingdom (London)	15	thermal oil Therminol VP-1	180/40	six different ORC configuration; WFs: sixteen working fluids	0.8–3 kW	two-tank configuration (high temperature, low temperature), buffer	Wang et al., 2021 [34]

4.3. Compound Parabolic Collectors (CPCs)

The implementation of CPC-ORC systems represents another well-researched alternative in the literature. The concentrator enhances solar radiation on the receiver, thereby improving performance. The CPC can function with or without tracking and primarily harnesses solar beam radiation while also capturing some diffuse solar irradiation. Typically, CPCs offer higher efficiency compared to ETCs, although they are more complex. In Table 4, the main parameters of the CPC-ORC units were shown.

Gang et al. [85] tested a regenerative ORC system composed of small concentration ratio CPC and combined with a heat storage made of PCM. The analysis examined the impact of heat regeneration on the system (collectors, ORC, and overall system efficiency), coming to the conclusion that the regenerative cycle had a positive effect on the efficiency of the ORC system and a negative effect on the efficiency of the collectors (due to the increase in the average working temperature of the first-stage collectors). Therefore, it is recommended to analyze the efficiency when considering regeneration in the ORC system. Wang et al. [86] investigated the off-design behavior of the ORC and CPC system, taking factors such as ambient temperature changes into account, vapor generator thermal oil mass flow rates and CPC. The off-design performance of the system throughout the day for various months was analyzed. Both a decrease in ambient temperature and an increase in thermal oil mass flow rates of the vapor generator and CPC were shown to improve the off-design performance. Villarini et al. [87] investigated and compared two small-scale solar-ORC trigeneration plants. The first plant consisted of compound parabolic collectors, an oil storage tank, an ORC plant, and an absorption chiller, while the second plant consisted of linear Fresnel reflectors (LFRs), a phase change material storage tank, an ORC unit, and the same absorption chiller. The higher condensing temperatures necessary in summer to supply the absorption chiller significantly limited the electrical efficiency of the solar CPC-ORC. However, the LFR technology allowed for the achievement of higher temperatures and conversion efficiencies in summer, making the solar CPC-ORC especially suitable for solar cooling applications. Bocci et al. [88] analyzed and integrated a tri-generation solar power plant, consisting of 50 m^2 of collectors, 3 m^3 of thermal storage, 3 kWe ORC, 8 kW absorber, and reverse osmosis desalination unit with a capacity of 200 L/h. Cioccolanti et al. [89] explored the potential of a small-scale concentrated solar-ORC plant coupled with an absorber. The study involves a simulation analysis of a 50 m^2 CPC solar field, a 3.5 kWe ORC, and a 17.6 kWc absorption chiller. The main objective of this work was to assess the performance of this integrated system and evaluate its feasibility for residential applications. In a different work by Cioccolanti et al. [90], a small-scale solar trigeneration system consisting of a small solar-ORC unit composed of a CPC and an absorption chiller was tested. The results showed that the appropriate setting of design parameters, especially the operating temperature range of the storage tanks, significantly affected the efficiency of the system. Antonelli et al. [91] presented a regenerative ORC (with CPC collectors). A numerical model was developed for the expansion machine derived from a modified Wankel engine, as well as a CPC model, to analyze the electricity generation in relation to ambient and operating conditions. The study was conducted for five working fluids. In another work, Antonelli et al. [92] developed the model of static CPC and an ORC system, using a rotary volumetric expander using AMESim, where all the main components of the plant were modeled. Results indicate that using a variable rotating speed volumetric expansion device enabled the plant to operate at various radiations and ambient temperatures without storage or external heat sources. Li and Li [93] introduced a genetic algorithm to optimize the performance of a small-scale SORC using solar radiation data for a typical year. The algorithm focuses on optimizing the evaporation temperature and thermal energy storage capacity, while aiming to improve power output and reduce power output fluctuations. Their analysis revealed that there was a minimum SORC scale required for profitability in a specific location, and increasing the system scale led to higher profit growth rates.

Table 4. An overview of the solar-ORC systems employing CPCs.

Region	Collector Area [m^2]	HTF	Operating Temperature [°C]	ORC System, Working Fluid	Power Output	TES Type	Authors (Year), Ref.
for locations with radiation: 600, 750, 900 W/m^2	output parameter	conduction oil	120/20	regenerative ORC; WF: HCFC-123	output parameter	thermal storage with PCMs	Gang et al., 2010 [85]
China (Xi'an city)	output parameter	thermal oil	N/A	simple ORC; WF: R245fa	output parameter	thermal storage tank with water	Wang et al., 2014 [86]
Italy (Napoli)	146	therminol 62	output parameters	small-scale regenerative solar ORC trigeneration plants: WF: R245fa	3.5 kWe	oil storage tank (3 m^3)	Villarini et al., 2019 [87]
Italy (Orte)	50	Therminol 62	150/30	simple ORC, WF: R245fa	1.8–3 kW	two tank storage system, 3 m^3 of thermal storage	Bocci et al., 2015 [88]
Italy (Orte)	50	Therminol 62	maximum evaporation temperature 150; minimum driving temperature difference between the evaporator and the condenser at the expander equal to 50 °C	regenerative ORC; WF: R245fa	3.5 kWe	two TES tanks: HTT used between the solar field and the ORC; LTT—the ORC thermal output and the absorber (3000 l each)	Cioccolanti et al., 2017 [89]
Italy (Orte)	50	HTT: diathermic oil LTT: water	100–150/15–30	simple ORC; WF: R245fa	3.5 kWe	two 3 m^3 heat storage tanks: HTT, LTT	Cioccolanti et al., 2018 [90]
Italy (Pisa)	750	pressurized water	100–120/output parameter	Regenerative ORC (with a modified Wankel engine); WF: R134a, R152a, R236ea, R245fa, R600a	50 kW	none	Antonelli et al., 2014 [91]
Italy (Pisa)	a surface of the panels of 197	pressurized water	150/condensing temperature was 15 °C higher than the ambient temperature	regenerative ORC (with rotary volumetric expander); WF: R600a	25 kW	none	Antonelli et al., 2016 [92]
Thailand (Bangkok)	2.16 per unit, respectively; 100 to 1200 units (with 50 units increment)	water	N/A	simple ORC; WF: R245fa	20, 40 and 60 kWe	none	Sonsaree et al., 2018 [77]
USA (Desert Rock, Nevada; Fort Peck, Montana; Pennsylvania State University, Pennsylvania; Bondville, Illinois)	output parameter: 5–565	water	Evaporation temperature: 390–430 K	simple ORC; WF: R245fa	output parameter	capacity of TES: 20–400 L	Li and Li, 2018 [93]

4.4. Parabolic Trough Collector (PTCs)

In this review, linear concentrating collectors are represented by the Parabolic Trough Collectors (PTCs), which can operate across a wide range of temperatures depending on the heat transfer fluid used. For example, with thermal oil, PTCs can function at temperatures of up to 400 °C, while with molten salt, they can reach even higher temperatures, up to 600 °C. More importantly, these collectors can be paired with the ORC systems that operate using a broad variety of working fluids and can also be integrated into artificial polygeneration systems. Artificial polygeneration systems refer to configurations that combine multiple energy production processes, such as electricity, heating, and cooling, within a single setup to improve overall system efficiency. In solar-driven Organic Rankine Cycle (ORC) systems, polygeneration often involves integrating ORC technology with solar energy and other renewable sources like geothermal or biomass. PTC-ORC systems are frequently used due to their technological maturity, moderate costs, flexibility, and relatively high performance for such systems [94]. Roumpedakis et al. [95] used multi-objective genetic algorithm optimization to analyze a small-scale ORC system with parabolic dish and trough (PTC) collectors derived for medium-to-high temperature (up to 210 °C). The optimization was carried out to maximize system efficiency and minimize the average cost of electricity produced. Up to 14 working factors were considered, and the optimization variables were the area of the solar field and the capacity of the storage tank. Installations located in the following five different European cities were considered: Athens, Madrid, Rome, Brussels, and Berlin. With the larger size of the system and the increased nominal heat load (80 kWth), it was more profitable to locate the installation in the south—Athens. Yu et al. [96] developed the optimal design and operation based on the PSO algorithm. For all the cases and working fluids, the use of recuperative ORC improved the thermal and the system efficiencies. Bellos and Tzivanidis (2021), [97] in their work, focused on investigating and optimizing a supercritical ORC with CO_2 as the working medium, which was directly heated inside the collectors (there was no secondary circulation loop between CO_2 and the collectors). Casartelli et al. [98] analyzed a 5MWel regenerative ORC system with toluene (first chosen in a simplified procedure) as the working fluid coupled to the linear solar collectors. The following two different solar technologies were considered: the parabolic trough collector and the linear Fresnel reflector. The analysis included the selection of design parameters and operating conditions and the calculation of the annual electricity production and the average cost of electricity on this basis. Research has shown that when the specific cost of a Fresnel-based plant is approximately half the cost of a parabolic trough collector, the levelized cost of electricity for Fresnel-based plants would be equivalent to that of the parabolic trough case. Chacartegui et al. [99] carried out a comparative analysis of two different thermal storage systems, namely the indirect system with Therminol VP-1 as HTF and the direct system with Hitec XL as HTF in 5 MW ORC system integrated with parabolic trough collectors. The study of Cau and Cocco [100] focused on the comparative analysis of medium-sized concentrating solar power plants (CSPs) based on an ORC unit integrated with parabolic trough collectors or linear Fresnel collectors. Evaluation of the efficiency of such systems has shown that CSP installations based on linear Fresnel collectors lead to higher values of electricity production per unit of occupied area. Manfrida et al. [101] performed a dynamic simulation of the operation of a solar-ORC unit connected to a latent heat storage (LHS) system with a storage containing PCM balls. The average weekly efficiency was obtained as 3.4% for the ORC system (3.9% for the whole unit).

The main parameters of the PTC-ORC unit are shown in the following table (Table 5).

Table 5. An overview of the solar-ORC system employing PTCs.

Region	Collector Area [m^2]	HTF	Operating Temperature [°C]	ORC System, Working Fluid	Power Output	TES Type	Authors (Year), Ref.
Belgium (Brussels), Greece (Athens), Spain (Madrid), Germany (Berlin) and Italy (Rome)	optimization variables: 10 ÷ 400	Therminol VP-1	210/>20	ORC system with recuperator; WFs: isohexane, acetone, hexane, cyclopentane, methanol, ethanol, heptane, cyclohexane, benzene, MDM, octane, toluene, n-nonane, p-xylene	output parameter	the thermal energy storage (TES); storage tank capacity—optimization variables: 0.2–5.0 m^3	Roumpedakis et al., 2021 [95]
China (Yinchuan)	from optimization	a mixture of Diphenyl Oxide and Biphenyl	independent variables in optimization: (300–400)/(50–300)—basic-ORC; (300–400)/(100–300)—recuperative ORC	basic and recuperative ORCs; WFs: toluene, cyclohexane, hexamethyldisiloxane (HMDSO), n-pentane, benzene and n-hexane	independent variables in optimization: 50—500 kW	sensible thermal energy storage system	Yu et al., 2021 [96]
Greece (Athens)	227.4	CO_2	default value: 800/25; Range: (600–1000)/(15–30) turbine inlet temp/condenser temp	recuperative ORC; WF: CO_2	44.14 kWe	none	Bellos and Tzivanidis, 2021 [97]
Greece (Athens, Thessaloniki), Turkey (Istanbul), Cyprus (Larnaca)—the South-East Mediterranean region:	optimization variable	water	110/90	a single stage conventional ORC; WFs: R134a, R245fa, R227ea, R152a, R236ea, R1234ze(E)	5 kW	storage tank	Roumpedakis et al., 2020 [71]
Spain (Sevilla)	output parameter	Therminol VP1	output parameter/40 °C	regenerative Rankine cycle; WF: toluene	5 MWel	none	Casartelli et al., 2015 [98]
Spain (Sevilla)	output parameters: for toluene varies between 38,400–77,200	Oil Therminol VP-1 in the indirect system; molten salt Hitec XL in a direct system	400/(30–120)	recuperative ORC; WFs: toluene, cyclohexane, siloxane D4	5 MWe	two different active storage systems: two tanks indirect storage system and two tanks direct storage system; output parameter: (0–10 h)	Chacartegui et al., 2016 [99]
India (Ahmadabad)	optimization variables: 200–5000	glycerol	275/161	regenerative solar-ORC, WF: isobutane	design capacity (power output): 50 kWe	a single-tank sensible heat storage system (optimization variables: storage hours 0–20 h)	Patil et al., 2017 [102]
Morocco (Fes, Errachidia, Oujda, Tata, Marrakech, Ouarzazate, and Benguerir)	design point area is equal to 10,496	Therminol VP-1	320/160	recuperative ORC, WF: cyclopentane	0–1.224 MWe under the considered weather conditions	a direct storage system (3 h)	Eddouibi et al., 2022 [103]
Senegal (isolated and arid rural settlement)	design outputs: 4703	Therminol VP-1	400/12	recuperative ORC; WF: cyclopentane	design outputs: 1018.41 kW	a direct storage system; storage capacity: 4 h volume of the storage tanks: 104 m^3	Sigue et al., 2022 [104]
USA (Crowley (Louisiana)	1051	water	121/93	WF: R245fa	0.05	buffer is planned	Chambers et al., 2014 [105]
Italy (Cagliari, Italy	865.5	Thermal oil	305/204	simple ORC; WF: a siliconic oil	1 MW	two-tank direct thermal storage system (storage capacity 4–12 h)	Cau and Cocco, 2014 [100]
Italy (Pisa San Giusto)	2583	water	120/70	simple ORC, WF: R245fa	output data	latent Heat Storage (LHS) system with PCH storage tank	Manfrida et al., 2016 [101]

5. Conclusions

This review has summarized the literature on the ORC systems driven by solar-thermal collectors, offering valuable insights into their performance, limitations, and future research directions.

This review highlights the evolution of solar-ORC systems, beginning with non-concentrating designs known for their simplicity and lower initial investment due to the absence of tracking mechanisms. Although these systems are cost-effective, their lower efficiency and the need for extensive collector areas to generate significant electricity limit their practical application. To address these limitations, research has increasingly focused on solar-concentrating systems integrated with ORC technology. Despite the fact that these systems are more complex and expensive due to the tracking mechanisms, they deliver significantly higher efficiencies, especially in regions with high direct solar irradiance. The transition to solar-concentrating systems represents a significant advancement in optimizing solar-ORC performance. These systems not only enhance energy capture but also reduce the land area required for effective electricity production. However, the current study reveals a significant research gap in the comprehensive analysis of ORC systems in temperate climates. While there is substantial research on the application of solar-ORC technologies in regions with high direct solar irradiance, investigations into their performance in temperate zones remain limited. In light of this, future research should address this gap by investigating the feasibility and performance of both concentrating and non-concentrating solar-ORC systems in temperate regions. Understanding how these systems perform under lower solar irradiance conditions is crucial for assessing their potential in diverse geographical settings. This includes evaluating their economic viability, operational challenges, and adaptations needed to optimize their performance in less sunny environments.

Linear concentrating systems, such as parabolic trough collectors, are particularly promising due to their ability to operate at high temperatures (up to 400–500 °C) while achieving good optical efficiency. Optical efficiency here refers to the effectiveness with which these systems capture and direct sunlight onto the receiver. This aspect is crucial as it influences how much of the incident solar energy is successfully concentrated and converted into thermal energy. Coupled with their strong thermal efficiency, which denotes their capability to convert captured solar energy into heat, PTCs offer a well-rounded performance for solar thermal applications. PTCs dominate the solar-ORC literature due to their maturity and performance under favorable solar conditions. In regions with lower solar resources or higher diffuse irradiance, evacuated tube collectors can perform comparably to PTCs at a lower cost and complexity.

Thermal energy storage is crucial for ensuring the continuous operation of solar-ORC systems, typically allowing energy storage for 4–8 h daily. While sensible heat storage is common practice, the use of phase change materials represents a significant advancement due to their ability to store and release energy more efficiently at varying temperatures. This approach has the potential to enhance the operational flexibility and efficiency of the solar-ORC systems.

Economic assessments indicate that solar-ORC systems can be more viable as part of broader polygeneration systems, particularly when coupled with concentrating collectors in locations with high solar potential. Although these systems have relatively high capital costs, technological advancements can reduce these costs over time. Compared to photovoltaic technology, solar-ORC systems incur higher initial costs but offer higher energy and exergy performance, along with the benefits of TES and polygeneration at a lower overall cost.

Among the different solar-ORC technologies, PTC-ORC systems are noted for their lower LCOE compared to PV technology of the same capacity. PTC systems are more promising, with an LCOE of approximately $0.18/kWh [106]. CPC-ORC systems have an LCOE of $0.21/kWh [77], making them a better choice than flat-plate collectors or ETCs.

Combining PTC with other renewables, such as geothermal or biomass, further reduces the LCOE to $0.15/kWh [107] and €0.10/kWh [108], respectively.

Despite their potential, solar-ORC systems face several technological limitations that require further research and development. High capital costs, particularly for small-scale applications, pose a significant barrier. Identifying high-performance turbines or expansion devices is essential to achieve high overall efficiencies, especially in small-scale systems, to make them financially competitive.

Another critical issue is the selection of high-performance working fluids that meet environmental standards, such as zero ozone depletion potential and low global warming potential, while maintaining high efficiency. This challenge has driven significant research efforts. For low-temperature systems, natural refrigerants like R290, R600, and R600a are promising, while for higher temperatures, fluids like toluene, cyclohexane, MDM (octamethyltrisiloxane), and MM (hexamethyldisiloxane) perform well. Comprehensive investigations into the optimal working fluids considering different application constraints remain necessary.

There is a significant need to expand the scope of research on underutilized solar collectors such as compound parabolic collectors and evacuated tube collectors, as both technologies have shown significant potential, especially in low- and medium-temperature applications. Although ETCs are often used due to their higher efficiency under diffuse radiation conditions and high thermal efficiency, their application in the context of ORC systems, especially with respect to the long-term operational stability and maintenance under variable climatic conditions, remains underexplored. On the other hand, CPCs offer a unique advantage of concentrating solar energy without the need for advanced tracking mechanisms, which can result in cost savings for decentralized energy systems. More focused studies are needed to fully understand their scalability, especially for small- and medium-scale projects, as well as their performance under different solar conditions to optimize their integration with ORC systems. The development of more efficient and scalable energy storage solutions remains a key area for further research, particularly to support the continuous operation of solar-ORC systems during periods of low solar radiance. While traditional thermal energy storage systems are widely used, research should be intensified on advanced alternatives such as phase change materials that can provide more stable and efficient thermal energy storage over a wider operating temperature range. In addition, the potential of thermocline storage using inexpensive materials such as rocks should be explored for larger-scale systems, providing a cost-effective way to store energy. Thermochemical storage, with its promise of long-term, inter-seasonal storage, offers possibility of storing excess energy produced during peak solar months for use during winter or periods of low solar irradiance, making it an ideal solution for solar-ORC applications. Feasibility studies on integrating these storage technologies into commercial ORC systems will be crucial for future developments. A major challenge for the future is to develop commercial solar-ORC systems that can compete with other power generation technologies and potentially replace fossil fuel-based systems. To achieve this, significant advancements in both the cost reduction and efficiency are necessary. One of the key obstacles is the current high capital cost of solar-ORC systems, which limits their widespread adoption, especially in regions where photovoltaic (PV) technologies are more economically viable. The development of more affordable components, such as high-efficiency turbines, will be essential to making solar-ORC systems competitive. In addition, improvements in the solar collectors, especially those that can operate efficiently in variable weather conditions and with lower maintenance costs, are crucial for solar-ORC system development. Research should focus on increasing the durability and thermal efficiency of collectors such as CPC and PTC, which offer better energy concentration but are currently associated with higher costs. Reducing the cost of materials for mirrors, reflectors, and absorbers, along with innovations in coatings that minimize heat loss, will also be key to increasing the overall efficiency and economic feasibility of solar-ORC systems. In addition, there should be a focus on scaling up experimental studies of full-scale systems under real-world conditions.

These studies will provide key data on the operational challenges, system longevity, and integration of solar-ORC into existing energy infrastructure. By addressing these issues, it will be possible to lay the foundation for cost-effective commercial products that can contribute to the transition away from fossil fuels, promoting a more sustainable energy future. In summary, the future directions of solar-ORC development should include a focus on the integration of advanced energy storage solutions, further research on working fluids for such systems, their operating parameters and selection methods, and the development of more cost-effective components. Expanding research on the performance of solar-ORC systems in different climatic conditions, especially in temperate and low-irradiance regions, will be crucial to broaden their application. In addition, the potential of polygeneration and hybrid systems, combining solar-ORC with other renewable technologies, should be further explored to increase efficiency and reduce costs. These advances will be essential to overcome the current technological and economic barriers, paving the way for the widespread commercial adoption of solar-ORC systems.

Funding: This research was funded by the Ministry of Science and Higher Education, Poland, grant AGH number 16.16.210.476.

Data Availability Statement: Data is contained within the article.

Conflicts of Interest: The author declares no conflict of interest.

Abbreviations

CPC	compound parabolic collector
DVG-ORC	direct vapor generated ORC
ETC	evacuated tube collector
FPC	flat plate collector
HRS	heat recovery system
HTF	heat transfer fluid
LCOE	levelized cost of electricity
LFR	Linear Fresnel Reflectors
MDM	octamethyltrisiloxane
MM	hexamethyldisiloxane
ORC	Organic Rankine Cycle
PCM	phase change materials
PEC	partial evaporation ORC
PSO	particle swarm optimization
PTC	parabolic through collector
PTC	solar Organic Rankine Cycle
SNORC	subcritical nonrecuperative ORC
SRORC	subcritical recuperative ORC
TES	thermal energy storage
TLC	trilateral ORC
TNORC	transcritical nonrecuperative ORC
TRORC	transcritical recuperative ORC
WF	working fluid

References

1. Huang, W.; Zheng, D.; Chen, X.; Shi, L.; Dai, X.; Chen, Y.; Jing, X. Standard Thermodynamic Properties for the Energy Grade Evaluation of Fossil Fuels and Renewable Fuels. *Renew. Energy* **2020**, *147*, 2160–2170. [CrossRef]
2. Piwowar, A.; Dzikuć, M. Development of Renewable Energy Sources in the Context of Threats Resulting from Low-Altitude Emissions in Rural Areas in Poland: A Review. *Energies* **2019**, *12*, 3558. [CrossRef]
3. Dzikuć, M.; Gorączkowska, J.; Piwowar, A.; Dzikuć, M.; Smoleński, R.; Kułyk, P. The Analysis of the Innovative Potential of the Energy Sector and Low-Carbon Development: A Case Study for Poland. *Energy Strategy Rev.* **2021**, *38*, 100769. [CrossRef]
4. Jullian, S.; Longaygue, X. From Conventional to More Sustainable Fuels: Trends and Needs in Research in the Thermodynamics Area. *Fluid. Phase Equilib.* **2014**, *362*, 192–195. [CrossRef]
5. Ceran, B. The Concept of Use of PV/WT/FC Hybrid Power Generation System for Smoothing the Energy Profile of the Consumer. *Energy* **2019**, *167*, 853–865. [CrossRef]

6. Forman, C.; Muritala, I.K.; Pardemann, R.; Meyer, B. Estimating the Global Waste Heat Potential. *Renew. Sustain. Energy Rev.* **2016**, *57*, 1568–1579. [CrossRef]
7. Rahimi, M.; Straub, A.P.; Zhang, F.; Zhu, X.; Elimelech, M.; Gorski, C.A.; Logan, B.E. Emerging Electrochemical and Membrane-Based Systems to Convert Low-Grade Heat to Electricity. *Energy Environ. Sci.* **2018**, *11*, 276–285. [CrossRef]
8. Shahverdi, K.; Loni, R.; Ghobadian, B.; Gohari, S.; Marofi, S.; Bellos, E. Numerical Optimization Study of Archimedes Screw Turbine (AST): A Case Study. *Renew. Energy* **2020**, *145*, 2130–2143. [CrossRef]
9. Olczak, P.; Olek, M.; Kryzia, D. The Ecological Impact of Using Photothermal and Photovoltaic Installations for DHW Preparation. *Energy Policy J.* **2020**, *23*, 65–74. [CrossRef]
10. Li, Z.; Lu, Y.; Huang, Y.; Qian, G.; Chen, F.; Yu, X.; Roskilly, A. Comparison Study of Trilateral Rankine Cycle, Organic Flash Cycle and Basic Organic Rankine Cycle for Low Grade Heat Recovery. *Energy Procedia* **2017**, *142*, 1441–1447. [CrossRef]
11. Rijpkema, J.; Munch, K.; Andersson, S.B. Thermodynamic Potential of Twelve Working Fluids in Rankine and Flash Cycles for Waste Heat Recovery in Heavy Duty Diesel Engines. *Energy* **2018**, *160*, 996–1007. [CrossRef]
12. Matuszewska, D.; Kuta, M.; Górski, J. The Environmental Impact of Renewable Energy Technologies Shown in Case of ORC-Based Geothermal Power Plant. *IOP Conf. Ser. Earth Environ. Sci.* **2019**, *214*, 012142. [CrossRef]
13. Iqbal, M.A.; Rana, S.; Ahmadi, M.; Date, A.; Akbarzadeh, A. Experimental Study on the Prospect of Low-Temperature Heat to Power Generation Using Trilateral Flash Cycle (TFC). *Appl. Therm. Eng.* **2020**, *172*, 115139. [CrossRef]
14. Demirkaya, G.; Padilla, R.V.; Fontalvo, A.; Lake, M.; Lim, Y.Y. Thermal and Exergetic Analysis of the Goswami Cycle Integrated with Mid-Grade Heat Sources. *Entropy* **2017**, *19*, 416. [CrossRef]
15. Demirkaya, G.; Padilla, R.V.; Fontalvo, A.; Bula, A.; Goswami, D.Y. Experimental and Theoretical Analysis of the Goswami Cycle Operating at Low Temperature Heat Sources. *J. Energy Resour. Technol.* **2018**, *140*, 072005. [CrossRef]
16. Modi, A.; Kærn, M.R.; Andreasen, J.G.; Haglind, F. Thermoeconomic Optimization of a Kalina Cycle for a Central Receiver Concentrating Solar Power Plant. *Energy Convers. Manag.* **2016**, *115*, 276–287. [CrossRef]
17. Masrur Hossain, M.; Afnan Ahmed, N.; Abid Shahriyar, M.; Monjurul Ehsan, M.; Riaz, F.; Salehin, S.; Awais Salman, C. Analysis and Optimization of a Modified Kalina Cycle System for Low-Grade Heat Utilization. *Energy Convers. Manag. X* **2021**, *12*, 100121. [CrossRef]
18. Manente, G. High Performance Integrated Solar Combined Cycles with Minimum Modifications to the Combined Cycle Power Plant Design. *Energy Convers. Manag.* **2016**, *111*, 186–197. [CrossRef]
19. Zaversky, F.; Les, I.; Sorbet, P.; Sánchez, M.; Valentin, B.; Brau, J.-F.; Siros, F. The Challenge of Solar Powered Combined Cycles—Providing Dispatchability and Increasing Efficiency by Integrating the Open Volumetric Air Receiver Technology. *Energy* **2020**, *194*, 116796. [CrossRef]
20. Ortiz, C.; Chacartegui, R.; Valverde, J.M.; Carro, A.; Tejada, C.; Valverde, J. Increasing the Solar Share in Combined Cycles through Thermochemical Energy Storage. *Energy Convers. Manag.* **2021**, *229*, 113730. [CrossRef]
21. Matuszewska, D.; Olczak, P. Evaluation of Using Gas Turbine to Increase Efficiency of the Organic Rankine Cycle (ORC). *Energies* **2020**, *13*, 1499. [CrossRef]
22. Yuksel, Y.E.; Ozturk, M.; Dincer, I. Thermodynamic Performance Assessment of a Novel Environmentally-Benign Solar Energy Based Integrated System. *Energy Convers. Manag.* **2016**, *119*, 109–120. [CrossRef]
23. Yılmaz, F. Thermodynamic Performance Evaluation of a Novel Solar Energy Based Multigeneration System. *Appl. Therm. Eng.* **2018**, *143*, 429–437. [CrossRef]
24. Özcan, Z.; Ekici, Ö. A Novel Working Fluid Selection and Waste Heat Recovery by an Exergoeconomic Approach for a Geothermally Sourced ORC System. *Geothermics* **2021**, *95*, 102151. [CrossRef]
25. Ziółkowski, P.; Hyrzyński, R.; Lemański, M.; Kraszewski, B.; Bykuć, S.; Głuch, S.; Sowiżdżał, A.; Pająk, L.; Wachowicz-Pyzik, A.; Badur, J. Different Design Aspects of an Organic Rankine Cycle Turbine for Electricity Production Using a Geothermal Binary Power Plant. *Energy Convers. Manag.* **2021**, *246*, 114672. [CrossRef]
26. Lecompte, S.; Oyewunmi, O.A.; Markides, C.N.; Lazova, M.; Kaya, A.; den Broek, M.; De Paepe, M. Case Study of an Organic Rankine Cycle (ORC) for Waste Heat Recovery from an Electric Arc Furnace (EAF). *Energies* **2017**, *10*, 649. [CrossRef]
27. Marchionni, M.; Fatigati, F.; Di Bartolomeo, M.; Di Battista, D.; Petrollese, M. Experimental and Numerical Dynamic Investigation of an ORC System for Waste Heat Recovery Applications in Transportation Sector. *Energies* **2022**, *15*, 9339. [CrossRef]
28. Mascuch, J.; Novotny, V.; Spale, J.; Vodicka, V.; Zeleny, Z. Experience from Set-up and Pilot Operation of an in-House Developed Biomass-Fired ORC Microcogeneration Unit. *Renew. Energy* **2021**, *165*, 251–260. [CrossRef]
29. Świerzewski, M.; Kalina, J.; Musiał, A. Techno-Economic Optimization of ORC System Structure, Size and Working Fluid within Biomass-Fired Municipal Cogeneration Plant Retrofitting Project. *Renew. Energy* **2021**, *180*, 281–296. [CrossRef]
30. Wang, M.; Jing, R.; Zhang, H.; Meng, C.; Li, N.; Zhao, Y. An Innovative Organic Rankine Cycle (ORC) Based Ocean Thermal Energy Conversion (OTEC) System with Performance Simulation and Multi-Objective Optimization. *Appl. Therm. Eng.* **2018**, *145*, 743–754. [CrossRef]
31. Hu, Z.; Fan, C.; Gao, W.; Chen, Y. Experimental Study of a Miniature Organic Rankine Cycle Unit Using Ocean Thermal Energy. *Energy Convers. Manag.* **2023**, *293*, 117494. [CrossRef]
32. Mikielewicz, D.; Mikielewicz, J. Criteria for Selection of Working Fluid in Low-Temperature ORC. *Chem. Process Eng.* **2016**, *37*, 429–440. [CrossRef]

33. Thurairaja, K.; Wijewardane, A.; Jayasekara, S.; Ranasinghe, C. Working Fluid Selection and Performance Evaluation of ORC. *Energy Procedia* **2019**, *156*, 244–248. [CrossRef]
34. Wang, Y.; Song, J.; Chatzopoulou, M.A.; Sunny, N.; Simpson, M.C.; Wang, J.; Markides, C.N. A Holistic Thermoeconomic Assessment of Small-Scale, Distributed Solar Organic Rankine Cycle (ORC) Systems: Comprehensive Comparison of Configurations, Component and Working Fluid Selection. *Energy Convers. Manag.* **2021**, *248*, 114618. [CrossRef]
35. Jankowski, M.; Klonowicz, P.; Borsukiewicz, A. Multi-Objective Optimization of an ORC Power Plant Using One-Dimensional Design of a Radial-Inflow Turbine with Backswept Rotor Blades. *Energy* **2021**, *237*, 121506. [CrossRef]
36. Jankowski, M. A New Indicator for Minimizing Size of an ORC Power Plant Based on Heat Exchanger and Turbine Design Parameters. *Appl. Therm. Eng.* **2022**, *201*, 117750. [CrossRef]
37. Alvi, J.Z.; Imran, M.; Pei, G.; Li, J.; Gao, G.; Alvi, J. Thermodynamic Comparison and Dynamic Simulation of Direct and Indirect Solar Organic Rankine Cycle Systems with PCM Storage. *Energy Procedia* **2017**, *129*, 716–723. [CrossRef]
38. Alvi, J.Z.; Feng, Y.; Wang, Q.; Imran, M.; Alvi, J. Modelling, simulation and comparison of phase change material storage based direct and indirect solar organic Rankine cycle systems. *Appl. Therm. Eng.* **2020**, *170*, 114780. [CrossRef]
39. History of ORC. Knowledge Center for Organic Rankine Cycle. Available online: https://kcorc.org/technology/history/ (accessed on 7 July 2024).
40. ORC World Map. Available online: https://orc-world-map.org/ (accessed on 7 July 2024).
41. Tartière, T.; Astolfi, M. A World Overview of the Organic Rankine Cycle Market. *Energy Procedia* **2017**, *129*, 2–9. [CrossRef]
42. Harinck, J.; Guardone, A.; Colonna, P. The Influence of Molecular Complexity on Expanding Flows of Ideal and Dense Gases. *Phys. Fluids* **2009**, *21*, 0036850420950130. [CrossRef]
43. Bao, J.; Zhao, L. A Review of Working Fluid and Expander Selections for Organic Rankine Cycle. *Renew. Sustain. Energy Rev.* **2013**, *24*, 325–342. [CrossRef]
44. Matuszewska, D.; Sztekler, K.; Gorski, J. An Influence of Low-Stability Region on Dense Gas Phenomena and Their Peculiarities in the ORC Fluids. *MATEC Web Conf.* **2014**, *18*, 03005. [CrossRef]
45. Tchanche, B.F.; Papadakis, G.; Lambrinos, G.; Frangoudakis, A. Fluid Selection for a Low-Temperature Solar Organic Rankine Cycle. *Appl. Therm. Eng.* **2009**, *29*, 2468–2476. [CrossRef]
46. Almehmadi, F.A.; Elattar, H.F.; Fouda, A.; Alqaed, S.; Mustafa, J.; Alharthi, M.A.; Refaey, H.A. Energy Performance Assessment of a Novel Solar Poly-Generation System Using Various ORC Working Fluids in Residential Buildings. *Energies* **2022**, *15*, 8286. [CrossRef]
47. Loni, R.; Najafi, G.; Asli-Ardeh, E.A.; Ghobadian, B.; Le Roux, W.G.; Yusaf, T. Performance Investigation of Solar ORC Using Different Nanofluids. *Appl. Sci.* **2019**, *9*, 3048. [CrossRef]
48. Jiang, Y.; Zhang, X.; Zhang, Z.; Hao, L.; Cao, Z.; Li, S.; Guo, B.; Zheng, Y.; Dong, C.; Zhao, L. Performance Evaluation and Working Fluid Screening of Direct Vapor Generation for Solar ORC Using Low-Global Warming Potential (GWP) Working Fluids. *Energies* **2024**, *17*, 3133. [CrossRef]
49. Rayegan, R.; Tao, Y.X. A Procedure to Select Working Fluids for Solar Organic Rankine Cycles (ORCs). *Renew. Energy* **2011**, *36*, 659–670. [CrossRef]
50. Lukawski, M.; Tester, J.; DiPippo, R. Impact of Molecular Structure of Working Fluids on Performance of Organic Rankine Cycles (ORCs). *Sustain. Energy Fuels* **2017**, *1*, 1098–1111. [CrossRef]
51. Petela, R. Exergy of Undiluted Thermal Radiation. *Sol. Energy* **2003**, *74*, 469–488. [CrossRef]
52. Siva Reddy, V.; Kaushik, S.C.; Ranjan, K.R.; Tyagi, S.K. State-of-the-Art of Solar Thermal Power Plants—A Review. *Renew. Sustain. Energy Rev.* **2013**, *27*, 258–273. [CrossRef]
53. Barber, R.E. Current Costs of Solar Powered Organic Rankine Cycle Engines. *Sol. Energy* **1978**, *20*, 1–6. [CrossRef]
54. Delcea, A.; Bitir-Istrate, I. Renewable Energy Sources for Industrial Consumers—A Past to Present Analysis of Technical and Financial Efficiency. *IOP Conf. Ser. Earth Environ. Sci.* **2021**, *664*, 12031. [CrossRef]
55. IEA Solar Heating & Cooling Programme. *SOLAR HEAT WORLD WIDE 2022*; IEA: Gleisdorf, Austria, 2023.
56. Karki, S.; Haapala, K.R.; Fronk, B.M. Technical and Economic Feasibility of Solar Flat-Plate Collector Thermal Energy Systems for Small and Medium Manufacturers. *Appl. Energy* **2019**, *254*, 113649. [CrossRef]
57. Pluta, Z. Evacuated Tubular or Classical Flat Plate Solar Collectors? *J. Power Technol.* **2011**, *91*, 158–164.
58. Sokhansefat, T.; Kasaeian, A.; Rahmani, K.; Heidari, A.H.; Aghakhani, F.; Mahian, O. Thermoeconomic and Environmental Analysis of Solar Flat Plate and Evacuated Tube Collectors in Cold Climatic Conditions. *Renew. Energy* **2018**, *115*, 501–508. [CrossRef]
59. Ersöz, M.A. Effects of Different Working Fluid Use on the Energy and Exergy Performance for Evacuated Tube Solar Collector with Thermosyphon Heat Pipe. *Renew. Energy* **2016**, *96*, 244–256. [CrossRef]
60. Olczak, P.; Olek, M. The Influence of Evacuated-Tube Collector Assembly on Heat Loss in Tracking Solar System with Parabolic Mirror Reflectors. *Proced. Eng.* **2016**, *157*, 317–324. [CrossRef]
61. Papadimitratos, A.; Sobhansarbandi, S.; Pozdin, V.; Zakhidov, A.; Hassanipour, F. Evacuated tube solar collectors integrated with phase change materials. *Sol. Energy* **2016**, *129*, 10–19. [CrossRef]
62. Zhang, D.; Diao, Y.; Wang, Z.; Pan, Y.; Sun, M.; Wang, X.; Du, P.; Zhao, Y. Thermal Performance of Two Evacuated Tube Solar Collectors with Flat Heat Pipes. *Appl. Therm. Eng.* **2024**, *241*, 122366. [CrossRef]

63. Ayompe, L.M.; Duffy, A.; Mc Keever, M.; Conlon, M.; McCormack, S.J. Comparative field performance study of flat plate and heat pipe evacuated tube collectors (ETCs) for domestic water heating systems in a temperate climate. *Energy* **2011**, *36*, 3370–3378. [CrossRef]
64. Olczak, P.; Porzuczek, J.; Kandefer, S. Passive Sun Tracking of a Single Evacuated Tube Collector with the Focusing Mirror. In Proceedings of the 2016 IEEE International Conference on Power and Renewable Energy, ICPRE, Shanghai, China, 21–23 October 2016.
65. Akrami, M.; Alsari, H.; Javadi, A.A.; Dibaj, M.; Farmani, R.; Fath, H.E.S.; Salah, A.H.; Negm, A. Analysing the Material Suitability and Concentration Ratio of a Solar-Powered Parabolic Trough Collector (PTC) Using Computational Fluid Dynamics. *Energies* **2020**, *13*, 5479. [CrossRef]
66. Chavarría-Domínguez, B.; De León-Aldaco, S.E.; Velázquez-Limón, N.; Ponce-Silva, M.; Aguilar-Jiménez, J.A.; Chavarría-Domínguez, F. A Review of the Modeling of Parabolic Trough Solar Collectors Coupled to Solar Receivers with Photovoltaic/Thermal Generation. *Energies* **2024**, *17*, 1582. [CrossRef]
67. Fernandez-Garcia, A.; Zarza, E.; Valenzuela, L.; Perez, M. Parabolic-trough solar collectors and their applications. *Renew. Sustain. Energy Rev.* **2010**, *14*, 1695–1721. [CrossRef]
68. Wang, M.; Wang, J.; Zhao, Y.; Zhao, P.; Dai, Y. Thermodynamic Analysis and Optimization of a Solar-Driven Regenerative Organic Rankine Cycle (ORC) Based on Flat-Plate Solar Collectors. *Appl. Therm. Eng.* **2013**, *50*, 816–825. [CrossRef]
69. Valencia Ochoa, G.; Ortiz, E.V.; Forero, J.D. Thermo-Economic and Environmental Optimization Using PSO of Solar Organic Rankine Cycle with Flat Plate Solar Collector. *Heliyon* **2023**, *9*, e13697. [CrossRef]
70. Ramos, A.; Chatzopoulou, M.A.; Freeman, J.; Markides, C.N. Optimisation of a High-Efficiency Solar-Driven Organic Rankine Cycle for Applications in the Built Environment. *Appl. Energy* **2018**, *228*, 755–765. [CrossRef]
71. Roumpedakis, T.C.; Loumpardis, G.; Monokrousou, E.; Braimakis, K.; Charalampidis, A.; Karellas, S. Exergetic and Economic Analysis of a Solar Driven Small Scale ORC. *Renew. Energy* **2020**, *157*, 1008–1024. [CrossRef]
72. Mavrou, P.; Papadopoulos, A.I.; Stijepovic, M.Z.; Seferlis, P.; Linke, P.; Voutetakis, S. Novel and Conventional Working Fluid Mixtures for Solar Rankine Cycles: Performance Assessment and Multi-Criteria Selection. *Appl. Therm. Eng.* **2015**, *75*, 384–396. [CrossRef]
73. Ancona, M.A.; Bianchi, M.; Branchini, L.; De Pascale, A.; Melino, F.; Peretto, A.; Poletto, C.; Torricelli, N. Solar Driven Micro-ORC System Assessment for Residential Application. *Renew. Energy* **2022**, *195*, 167–181. [CrossRef]
74. Habka, M.; Ajib, S. Performance Estimation of Mixtures in Solar Organic Rankine Cycle with Two Mini Cogeneration Options for Improvement Purpose. *Sustain. Energy Technol. Assess.* **2016**, *16*, 174–189. [CrossRef]
75. Alvi, J.Z.; Jinghu, Y.; Feng, Y.; Asim, M.; Qian, W.; Pei, G. Performance Assessment of Direct Vapor Generation Solar Organic Rankine Cycle System Coupled with Heat Storage. *Sustainability* **2022**, *14*, 15296. [CrossRef]
76. Rodriguez-Pastor, D.A.; Becerra, J.A.; Chacartegui, R. Adaptation of Residential Solar Systems for Domestic Hot Water (DHW) to Hybrid Organic Rankine Cycle (ORC) Distributed Generation. *Energy* **2023**, *263*, 125901. [CrossRef]
77. Sonsaree, S.; Asaoka, T.; Jiajitsawat, S.; Aguirre, H.; Tanaka, K. A Small-Scale Solar Organic Rankine Cycle Power Plant in Thailand: Three Types of Non-Concentrating Solar Collectors. *Sol. Energy* **2018**, *162*, 541–560. [CrossRef]
78. Kutlu, C.; Li, J.; Su, Y.; Pei, G.; Riffat, S. Off-Design Performance Modelling of a Solar Organic Rankine Cycle Integrated with Pressurized Hot Water Storage Unit for Community Level Application. *Energy Convers. Manag.* **2018**, *166*, 132–145. [CrossRef]
79. Twomey, B.; Jacobs, P.A.; Gurgenci, H. Dynamic Performance Estimation of Small-Scale Solar Cogeneration with an Organic Rankine Cycle Using a Scroll Expander. *Appl. Therm. Eng.* **2013**, *51*, 1307–1316. [CrossRef]
80. Piñerez, G.P.; Valencia Ochoa, G.; Duarte-Forero, J. Energy, Exergy, and Environmental Assessment of a Small-Scale Solar Organic Rankine Cycle Using Different Organic Fluids. *Heliyon* **2021**, *7*, e07947. [CrossRef]
81. Gilani, H.A.; Hoseinzadeh, S.; Esmaeilion, F.; Memon, S.; Garcia, D.A.; Assad, M.E.H. A Solar Thermal Driven ORC-VFR System Employed in Subtropical Mediterranean Climatic Building. *Energy* **2022**, *250*, 123819. [CrossRef]
82. Bellos, E.; Lykas, P.; Tzivanidis, C. Investigation of a Solar-Driven Organic Rankine Cycle with Reheating. *Appl. Sci.* **2022**, *12*, 2322. [CrossRef]
83. Scardigno, D.; Fanelli, E.; Viggiano, A.; Braccio, G.; Magi, V. A Genetic Optimization of a Hybrid Organic Rankine Plant for Solar and Low-Grade Energy Sources. *Energy* **2015**, *91*, 807–815. [CrossRef]
84. Atiz, A.; Karakilcik, H.; Erden, M.; Karakilcik, M. Assessment of Electricity and Hydrogen Production Performance of Evacuated Tube Solar Collectors. *Int. J. Hydrogen Energy* **2019**, *44*, 14137–14144. [CrossRef]
85. Pei, G.; Li, J.; Ji, J. Analysis of Low Temperature Solar Thermal Electric Generation Using Regenerative Organic Rankine Cycle. *Appl. Therm. Eng.* **2010**, *30*, 998–1004. [CrossRef]
86. Wang, J.; Yan, Z.; Zhao, P.; Dai, Y. Off-Design Performance Analysis of a Solar-Powered Organic Rankine Cycle. *Energy Convers. Manag.* **2014**, *80*, 150–157. [CrossRef]
87. Villarini, M.; Tascioni, R.; Arteconi, A.; Cioccolanti, L. Influence of the Incident Radiation on the Energy Performance of Two Small-Scale Solar Organic Rankine Cycle Trigenerative Systems: A Simulation Analysis. *Appl. Energy* **2019**, *242*, 1176–1188. [CrossRef]
88. Bocci, E.; Villarini, M.; Vecchione, L.; Sbordone, D.; Di Carlo, A.; Dell'Era, A. Energy and Economic Analysis of a Residential Solar Organic Rankine Plant. *Energy Procedia* **2015**, *81*, 558–568. [CrossRef]

89. Cioccolanti, L.; Villarini, M.; Tascioni, R.; Bocci, E. Performance Assessment of a Solar Trigeneration System for Residential Applications by Means of a Modelling Study. *Energy Procedia* **2017**, *126*, 445–452. [CrossRef]
90. Cioccolanti, L.; Tascioni, R.; Bocci, E.; Villarini, M. Parametric Analysis of a Solar Organic Rankine Cycle Trigeneration System for Residential Applications. *Energy Convers. Manag.* **2018**, *163*, 407–419. [CrossRef]
91. Antonelli, M.; Baccioli, A.; Francesconi, M.; Lensi, R.; Martorano, L. Analysis of a Low Concentration Solar Plant with Compound Parabolic Collectors and a Rotary Expander for Electricity Generation. *Energy Procedia* **2014**, *45*, 170–179. [CrossRef]
92. Antonelli, M.; Baccioli, A.; Francesconi, M.; Desideri, U. Dynamic Modelling of a Low-Concentration Solar Power Plant: A Control Strategy to Improve Flexibility. *Renew. Energy* **2016**, *95*, 574–585. [CrossRef]
93. Li, S.; Li, W. Thermo-Economic Optimization of Solar Organic Rankine Cycle Based on Typical Solar Radiation Year. *Energy Convers. Manag.* **2018**, *169*, 78–87. [CrossRef]
94. Loni, R.; Mahian, O.; Markides, C.N.; Bellos, E.; le Roux, W.G.; Kasaeian, A.; Najafi, G.; Rajaee, F. A Review of Solar-Driven Organic Rankine Cycles: Recent Challenges and Future Outlook. *Renew. Sustain. Energy Rev.* **2021**, *150*, 111410. [CrossRef]
95. Roumpedakis, T.C.; Fostieris, N.; Braimakis, K.; Monokrousou, E.; Charalampidis, A.; Karellas, S. Techno-Economic Optimization of Medium Temperature Solar-Driven Subcritical Organic Rankine Cycle. *Thermo* **2021**, *1*, 77–105. [CrossRef]
96. Yu, H.; Helland, H.; Yu, X.; Gundersen, T.; Sin, G. Optimal Design and Operation of an Organic Rankine Cycle (ORC) System Driven by Solar Energy with Sensible Thermal Energy Storage. *Energy Convers. Manag.* **2021**, *244*, 114494. [CrossRef]
97. Bellos, E.; Tzivanidis, C. Investigation of a Novel CO_2 Transcritical Organic Rankine Cycle Driven by Parabolic Trough Solar Collectors. *Appl. Syst. Innov.* **2021**, *4*, 53. [CrossRef]
98. Casartelli, D.; Binotti, M.; Silva, P.; Macchi, E.; Roccaro, E.; Passera, T. Power Block Off-Design Control Strategies for Indirect Solar ORC Cycles. *Energy Procedia* **2015**, *69*, 1220–1230. [CrossRef]
99. Chacartegui, R.; Vigna, L.; Becerra, J.A.; Verda, V. Analysis of Two Heat Storage Integrations for an Organic Rankine Cycle Parabolic Trough Solar Power Plant. *Energy Convers. Manag.* **2016**, *125*, 353–367. [CrossRef]
100. Cau, G.; Cocco, D. Comparison of Medium-Size Concentrating Solar Power Plants Based on Parabolic Trough and Linear Fresnel Collectors. *Energy Procedia* **2014**, *45*, 101–110. [CrossRef]
101. Manfrida, G.; Secchi, R.; Stańczyk, K. Modelling and Simulation of Phase Change Material Latent Heat Storages Applied to a Solar-Powered Organic Rankine Cycle. *Appl. Energy* **2016**, *179*, 378–388. [CrossRef]
102. Patil, V.R.; Biradar, V.I.; Shreyas, R.; Garg, P.; Orosz, M.S.; Thirumalai, N.C. Techno-Economic Comparison of Solar Organic Rankine Cycle (ORC) and Photovoltaic (PV) Systems with Energy Storage. *Renew. Energy* **2017**, *113*, 1250–1260. [CrossRef]
103. Eddouibi, J.; Abderafi, S.; Vaudreuil, S.; Bounahmidi, T. Dynamic Simulation of Solar-Powered ORC Using Open-Source Tools: A Case Study Combining SAM and Coolprop via Python. *Energy* **2022**, *239*, 121935. [CrossRef]
104. Sigue, S.; Abderafi, S.; Vaudreuil, S.; Bounahmidi, T. Design and Steady-State Simulation of a CSP-ORC Power Plant Using an Open-Source Co-Simulation Framework Combining SAM and DWSIM. *Therm. Sci. Eng. Prog.* **2023**, *37*, 101580. [CrossRef]
105. Chambers, T.; Raush, J.; Russo, B. Installation and Operation of Parabolic Trough Organic Rankine Cycle Solar Thermal Power Plant in South Louisiana. *Energy Procedia* **2014**, *49*, 1107–1116. [CrossRef]
106. Khalid, F.; Dincer, I.; Rosen, M.A. Techno-Economic Assessment of a Renewable Energy Based Integrated Multigeneration System for Green Buildings. *Appl. Therm. Eng.* **2016**, *99*, 1286–1294. [CrossRef]
107. Heberle, F.; Hofer, M.; Ürlings, N.; Schröder, H.; Anderlohr, T.; Brüggemann, D. Techno-Economic Analysis of a Solar Thermal Retrofit for an Air-Cooled Geothermal Organic Rankine Cycle Power Plant. *Renew. Energy* **2017**, *113*, 494–502. [CrossRef]
108. Pantaleo, A.M.; Camporeale, S.M.; Sorrentino, A.; Miliozzi, A.; Shah, N.; Markides, C.N. Solar/Biomass Hybrid Cycles with Thermal Storage and Bottoming ORC: System Integration and Economic Analysis. *Energy Procedia* **2017**, *129*, 724–731. [CrossRef]